In Vivo Photovoltaic Performance of a Silicon Nanowire Photodiode–Based Retinal Prosthesis

Brandon Bosse,[1] Samir Damle,[2] Abraham Akinin,[2] Yi Jing,[1] Dirk-Uwe Bartsch,[3] Lingyun Cheng,[3] Nicholas Oesch,[3,4] Yu-Hwa Lo,[5] Gert Cauwenberghs,[2] and William R. Freeman[3]

[1]Nanovision Biosciences, Inc., La Jolla, California, United States
[2]Department of Bioengineering, University of California, San Diego, California, United States
[3]Jacobs Retina Center at Shiley Eye Institute, Department of Ophthalmology, University of California, San Diego, California, United States
[4]Department of Psychology, University of California, San Diego, California, United States
[5]Department of Electrical and Computer Engineering, University of California, San Diego, California, United States

PURPOSE. For more than 20 years, there has been an international, multidisciplinary effort to develop retinal prostheses to restore functional vision to patients blinded by retinal degeneration. We developed a novel subretinal prosthesis with 1512 optically addressed silicon nanowire photodiodes, which transduce incident light into an electrical stimulation of the remaining retinal circuitry. This study was conducted to evaluate the efficacy of optically driving the subretinal prosthesis to produce visual cortex activation via electrical stimulation of the retina.

METHODS. We measured electrically evoked potential responses (EEPs) in rabbit visual cortex in response to illumination of the subretinal nanowire prosthesis with pulsed 852-nm infrared (IR) light. We compared the EEP responses to visually evoked potential responses (VEPs) to pulsed 532-nm visible light (positive control) and pulsed 852-nm IR light (negative control).

RESULTS. Activating the devices with IR light produced EEP responses with a significantly higher trough-to-peak amplitude (54.17 ± 33.4 µV) than IR light alone (24.07 ± 22.1 µV) or background cortical activity (23.22 ± 17.2 µV). EEP latencies were significantly faster than focal VEP latencies. Focal VEPs produced significantly higher amplitudes (94.88 ± 43.3 µV) than EEPs. We also demonstrated how an electrode placed on the cornea can be used as a noninvasive method to monitor the function of the implant.

CONCLUSIONS. These results show that subretinal electrical stimulation with nanowire electrodes can elicit EEPs in the visual cortex, providing evidence for the viability of a subretinal nanowire prosthetic approach for vision restoration.

Keywords: retinal prosthesis, implant, nanowires, in vivo, rabbit

Retinitis pigmentosa and AMD are debilitating causes of blindness resulting from the gradual loss of photoreceptors in the outer retina. It is estimated that more than one million people worldwide are blinded by retinitis pigmentosa,[1] and it is projected that there will be 196 million people with AMD by 2020.[2] Available treatments slow the progress of the degeneration but do not reverse vision loss. In these diseases, only the photoreceptor layer degenerates, leaving the remainder of the retina intact,[3] albeit with some remodeling.[4] Retinal prosthetics function by electrically stimulating spared retina, bypassing the missing photosensory neurons. This approach makes use of the remaining visual pathway to elicit phosphenes in a retinotopic manner to restore some useful vision to the patient.

There are three retinal prostheses that are available to patients in the European Economic Area having been granted the CE mark for commercial use: Retina Implant Alpha AMS subretinal implant with 1600 electrodes at 70-µm pitch (Retina Implant AG, Reutlingen, Germany),[5,6] IRIS II epiretinal implant with 150 electrodes (Pixium Vision, Paris, France),[7] and Argus II epiretinal implant (Second Sight Medical Products, Inc., Sylmar, CA, USA).[8] Of those, only the Argus II device is also approved by the US Food and Drug Administration (FDA) and available to patients in the US market, but its 60 electrodes at 525-µm electrode pitch results in stimulation being spread over a large field of view, precluding high-resolution vision. Recently, Retina Implant AG and Pixium Vision have commenced clinical trials in the United States for their latest devices, Alpha AMS[9] and PRIMA[10] (378 photovoltaic electrodes, 70-µm pitch).[11-16] A major goal of retinal prosthetic development is to decrease pixel spacing and increase pixel number to improve high acuity vision over a larger area of the visual field.

We developed a retinal prosthesis with a high-resolution subretinal neurostimulator consisting of 1512 optically addressed silicon nanowire photodiodes.[17] Each nanowire photodiode converts incident light into electric current to stimulate nearby inner retinal neurons, which allows for a compact, optically addressable stimulating array and obviates the need for individually wired electrodes. There are several key advantages to implanting the device in the subretinal space. Specifically, it avoids direct activation of retinal ganglion cell axons in the retinal fiber layer, which can cause streaked
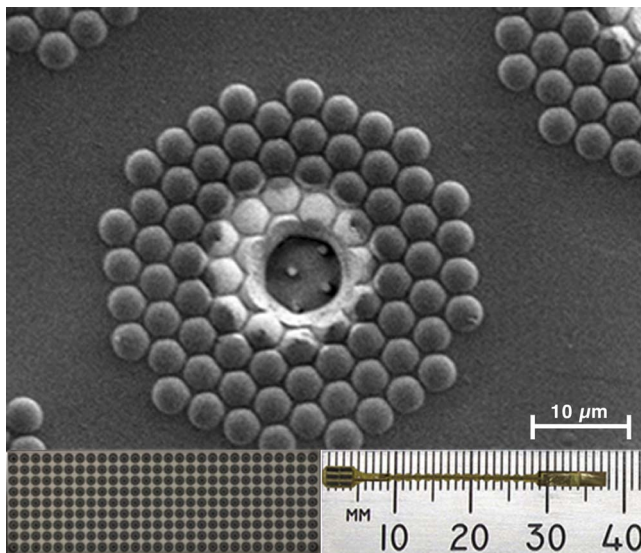
FIGURE 1. The retinal prosthesis consists of six tiles on a polyimide substrate (*bottom right*). Each tile has 252 electrodes (*bottom left*). Each of the electrodes has 85 silicon nanowires capped with iridium oxide (*top*).

FIGURE 2. Fundus photograph showing retina covering the six-tiled nanowire implant following surgical placement into the subretinal space.

phosphenes.[18] It also makes use of remaining inner retinal circuitry, allowing for more natural image processing.

In vivo electrophysiology studies are essential to demonstrate that an implant effectively stimulates the retina to generate neural signals that are transmitted to the visual cortex as in natural vision. Recording visually evoked potentials (VEPs) from the occipital cortex in response to repeated visual stimuli is a common clinical measure of visual pathway integrity.[19] This technique can be extended to record electrically evoked potentials (EEPs) to demonstrate the effectiveness of prosthetics to electrically stimulate the retina and cause a cortical response in the visual cortex.[20–31] In vivo studies also allow for optimization of surgical technique and biocompatibility evaluation of the retinal prosthetic device in an animal model. Here, we use an in vivo rabbit model to demonstrate the effectiveness of subretinal stimulation with a nanowire prosthesis and compare the visible light–induced VEP response with the EEP response to prosthetic stimulation.

METHODS

Photovoltaic Implants

The silicon nanowire photovoltaic devices were fabricated using the procedures as previously described.[17] The subretinal implants consisted of six silicon tiles mounted onto a flexible polyimide substrate (Fig. 1, bottom right), covering an area of 3 × 4 mm, or approximately 17° of visual field. Each tile measured 1.4 × 0.5 mm and contained an array of 252 sputtered iridium oxide film (SIROF) electrodes with a diameter of 12 μm and spaced with a pitch of 50 μm (Fig. 1, bottom left) for a total of 1512 stimulating electrodes. Each electrode consisted of a group of 85 vertically aligned silicon p-n junction nanowires (Fig. 1, top), bundled together under a transparent indium tin oxide electrode. Through the photovoltaic effect, the nanowires convert the energy of the incident light into an electron-hole electrical charge pair, as a typical photodiode.[32–35] Each nanowire electrode pixel is coated with parylene and capped with a SIROF electrode located in the center of the pixel, which delivers the charge to the retina. The stimulating electrodes 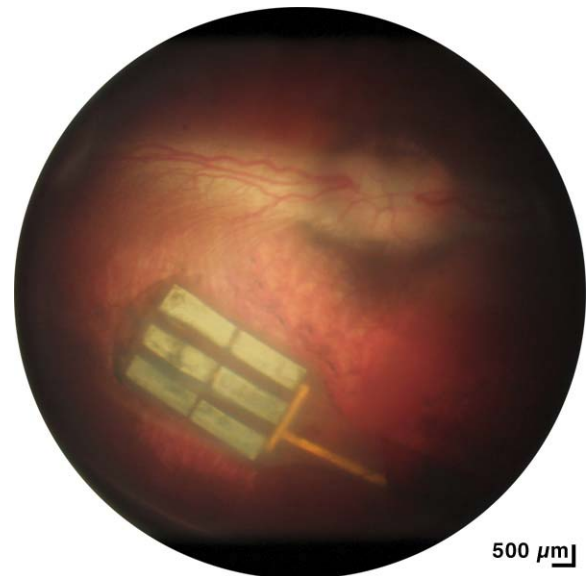shared a common return electrode located 6 mm away from the stimulating electrodes. In this study, the devices were unbiased and powered only with high-intensity infrared (IR) light described later. Each implant was sterilized in a steam autoclave (Tuttnauer, Hauppauge, NY, USA) for 7 minutes at 31 PSI and 134°C.

Device Implantation Surgery

New Zealand pigmented rabbits ($N = 12$; average age, 4.9 months; 4.1 kg) were implanted with a subretinal prosthesis in this study. All experimental methods and animal care procedures adhered to the ARVO Statement for the Use of Animals in Ophthalmic and Vision Research and were approved by the University of California, San Diego, Institutional Animal Care and Use Committee. Anesthesia was induced by a cocktail of ketamine hydrochloride (35 mg/kg) and xylazine (5 mg/kg) administered by subcutaneous injection and maintained with alternating half-doses of ketamine only or ketamine and xylazine every 30 to 40 minutes. The pupils were dilated with 1% atropine, 0.5% tropicamide, and 2.5% phenylephrine. Implantation of the device was performed using a trans-scleral (i.e., ab externo) approach unilaterally in the right eye. Two polyimide glides were used to support the device on both sides as it was inserted into the subretinal space. The head of the device containing the stimulating electrode array was placed near the visual streak. The tail of the implant was anchored at the scleral incision by a 7-0 nylon suture. After insertion, a 25-gauge three-port trans pars plana vitrectomy was performed before air–fluid exchange and final tamponade with silicon oil (ADATO SIL-ol 5000; Bausch & Lomb, Rochester, NY, USA). The vitrectomy was performed using a Landers wide field vitrectomy lens under a surgical microscope (Zeiss, Oberkochen, Germany). Fundus photographs (Fig. 2) and optical coherence tomography (OCT; Fig. 3) were taken the following day to verify implant position.

Cortical Electrode Implantation Surgery

The day following implantation surgery, the rabbit was implanted with cortical recording electrodes as previously described.[27,36] The rabbit was anesthetized as described above,
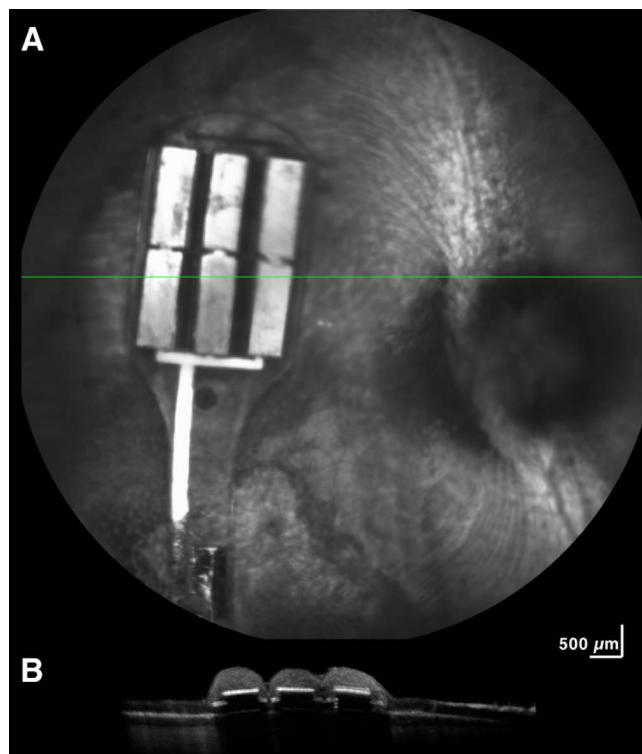
FIGURE 3. OCT imaging 24 hours after implantation shows that retina overlaying the device is in close contact with the retinal prosthesis tiles. The *horizontal line* across the prosthesis (**A**) corresponds to the cross section of retina over the tiles shown below (**B**).

and the skin over the posterior skull was prepared by shaving the scalp with electric clippers. The skin was incised, the periosteum was opened, and the skull was exposed. Two skull burr holes were made with a 1.5-mm surgical drill 5 mm away from the sagittal suture on each side overlying the visual cortex and 6 mm anterior to lambda. A third burr hole was made for the reference electrode 3 mm right of the sagittal suture and 5 mm anterior to bregma (Fig. 4). A grounding electrode was placed on the ear. Subsequently, 4.75-mm cranial screw electrodes were inserted until achieving contact with the dura. Dental cement was then applied and cured to hold the electrodes securely in place and the incision was closed by suturing.

Light Stimulation Delivery

A Large Spot slit-lamp adapter (Iridex Corp., Mountain View, CA, USA) was used to project a 3-mm-diameter laser through a slit-lamp (Haag-Streit, Mason, OH, USA) into the eye. Two laser diodes (DJ532-40 and L852P150; Thorlabs, Newton, NJ, USA) were used to emit 10-ms pulses every 500 ms of either 532-nm 100-μW/mm^2 green light or 852-nm 3.4-mW/mm^2 infrared light. Green 532-nm light was used as a positive control to verify natural VEPs were elicited from retina over the implant. Although the device is sensitive to both visible and IR light, we used 852-nm IR light to activate the device to avoid natural stimulation of the rabbit photoreceptors. The laser diodes were mounted in a temperature-controlled mount (TCLDM9; Thorlabs) and driven by a Benchtop Laser Controller (ITC4020; Thorlabs). In patients, a glasses-mounted camera will capture the visual scene and project patterns of IR light into the implanted eye via a DLP pico display (Texas Instruments, Dallas, TX, USA) while still permitting visible light to pass through allowing for residual natural vision.
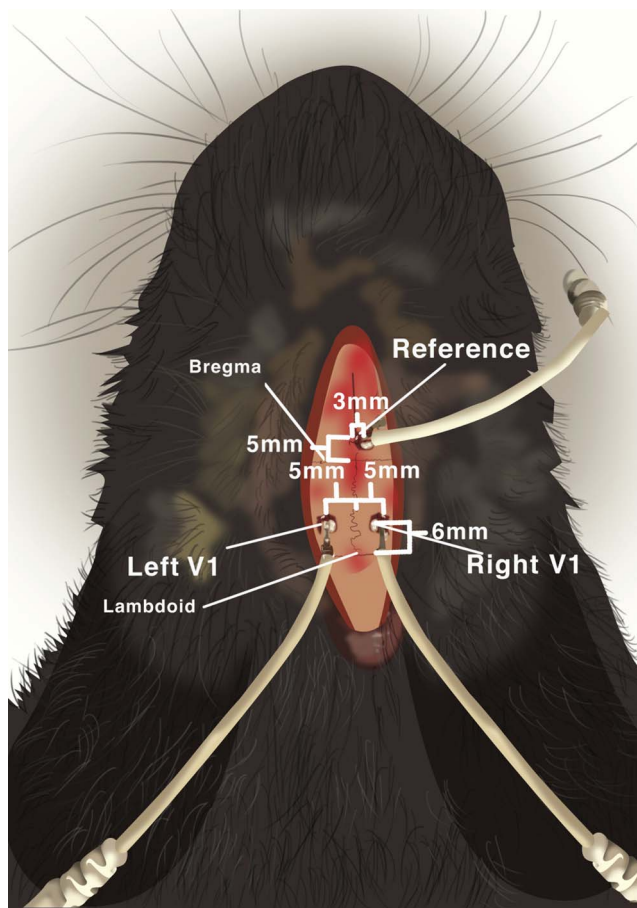

FIGURE 4. Cortical screw electrode placement diagram demonstrating electrode locations with respect to skull suture landmarks in the rabbit.

Electrophysiology Recording

Electrophysiology measurements were recorded using an animal physiology UBA-4204 Universal Biomedical Amplifier (LKC Technologies, Gaithersburg, MD, USA) at 2-kHz sampling rate. A low-cut filter at 1 Hz, high-cut filter at 100 Hz, and notch filter at 60 Hz were applied to reduce ambient electrical noise. Unrelated cortical activity and noise were further minimized by averaging trial repeats (50 to 200) for each experimental condition. A HK Loop ERG electrode (Unimed Electrode Supplies, Farnham, UK) was placed on the cornea to monitor the device electrical activation, and a reference electrode was placed on the nose. Data were recorded for 256 ms every 500 ms. Following electrophysiology recordings, anesthetized animals were euthanized by an intracardiac injection of 120 mg sodium pentobarbital/kg body weight. After euthanasia, the eyes were enucleated and processed for histologic analysis by light microscopy.

Data Analysis

Data were imported into MATLAB (The Mathworks, Inc., Natick, MA, USA) for visualization and analysis. The baseline, measured at the first point, was subtracted from each trace such that all recordings began at 0 V. The amplitude of the N1 was measured at the lowest local minimum between time 20 and 60 ms after the start of the laser pulse. The start of the N1 time window was set at 20 ms to exclude the stimulation artifact. We used 60 ms as the end of the N1 time window based on the existing literature and preliminary data. P2 was
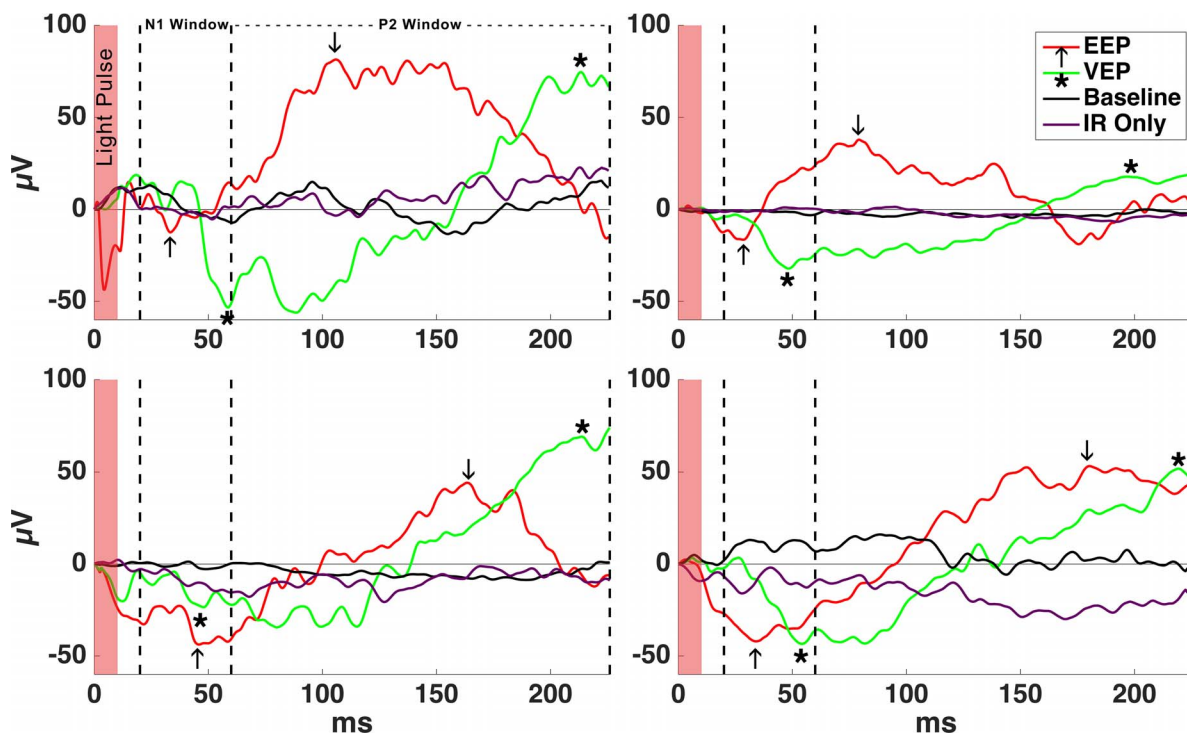
Figure 5. Example EEPs from four rabbits in response to electrical stimulation of the retina as the subretinal implant was activated with a 10-ms pulse of IR light over 50 repeats averaged. EEP N1 and P2 are marked with *arrows* (↑). Example VEPs in response to focal green stimulation are shown for comparison. VEP N1 and P2 are marked with *asterisks* (*). No VEPs were detected in response to 10-ms pulsed IR light in the nonimplanted eye, which resulted in a signal similar to baseline cortical activity without stimulation.

measured at the highest local maximum between 60 ms and the end of the recording. Local extrema were determined with the findpeaks MATLAB function. The VEP and EEP amplitudes were calculated from N1 trough to P2 peak. Latency of N1 and P2 was calculated from the start of the onset of the laser pulse. A total of 229 cortical recordings were made from seven rabbits (14 eyes): 108 recordings (from 7 eyes) of IR laser on the device-inducing EEPs, 45 recordings (from 7 eyes) of focal green laser–inducing VEPs in the implanted eye, 54 (from 7 eyes) recordings of baseline cortical activity without stimulation, and 22 (from 4 eyes) recordings of IR laser stimulation in the nonimplanted eye. Corneal potentials were recorded from six rabbits.

For the statistical analysis, a mixed model regression was performed using the VEP and EEP amplitudes as the dependent variable and recording conditions (four groups) as the independent variable while assigning the animal ID as a random effect to account for the repeated measurements. After identification of a significant association between amplitude and recording conditions, further comparisons of the least square means of amplitude among the four recording conditions were performed using the Student *t*-test while limiting type I errors to a rate of 0.05. The statistical analysis was performed using JMP SAS software version 13 (JMP, Cary, NC, USA).

RESULTS

EEPs

To examine how stimulation of the prosthetic device activates retina, EEPs were recorded by activating the subretinal prosthesis with a 10-ms pulse, 3-mm-diameter spot size, and 852-nm IR laser with an intensity of 3.4 mW/mm^2, resulting in

a charge injection of 0.32 nC per electrode; 852-nm light activates the prosthesis with high efficiency but does not activate mammalian photoreceptors.[37] IR stimulation of the device resulted in a voltage waveform on the contralateral electrode with a negative peak (N1) after stimulation followed by a positive peak (P2), consistent with activation of the visual cortex (Fig. 5). The average EEP amplitude from 108 recordings was 54.17 µV (SD = 33.4) and average N1 latency was 36.55 ms (SD = 11.6; Table; Fig. 6).

To determine whether high intensity IR light could directly activate photoreceptors and cause a VEP without prosthetic stimulation, we pulsed 852-nm light in the nonimplanted eye at the same intensity and duration. The nonimplanted eye was used instead of focusing the laser spot on retina away from the device to eliminate the possibility of activating the device with scattered light from the high-powered laser. No VEP waveform was observed from IR stimulation in nonimplanted eyes, and the average trough-to-peak amplitude of cortical activity in response to pulsed IR light stimulation was not significantly different from baseline cortical activity recordings in the absence of any stimulation (Fig. 6).

Focal VEPs Elicited From Retina Over the Device

To examine how implantation of the prosthetic device may influence normal responses of the retina, we stimulated the implanted eye with a visual stimulus using a 3-mm-diameter spot of 532-nm laser pulsed for 10 ms at 2 Hz. From a total of 45 recordings, the average focal VEP amplitude was 94.88 ± 43.3 µV (SD) and average N1 latency was 48.04 ± 12.3 ms (SD). Implanted eyes remained sensitive to visible light after implantation, exhibiting normal VEP waveform kinetics. The VEP amplitudes were greater than EEP amplitudes ($P < 0.0001$), and EEP N1 latencies were significantly faster than VEP N1 latencies by an average of 11.5 ms ($P < 0.0001$).

TABLE. Cortical Potential Amplitude Averages and Experimental Group Comparisons

Experimental condition	Focal green VEP	Device-elicited EEP	IR in nonimplanted eye	Baseline activity
Number of recordings	$n = 45$	$n = 108$	$n = 22$	$n = 54$
Cortical potential amplitude	Average = 94.88 µV	Average = 54.17 µV	Average = 24.07 µV	Average = 23.22 µV
Standard deviation	SD = 43.3	SD = 33.4	SD = 22.1	SD = 17.2
Baseline activity	$P < 0.0001$	$P < 0.0001$	$P = 0.8827$	
IR in Nonimplanted eye	$P < 0.0001$	$P < 0.0001$		
Device-elicited EEP	$P < 0.0001$			

The average VEP elicited by focal green stimulation was significantly higher than all other conditions (column 1). The average EEP elicited by device activation was significantly higher than both baseline activity and IR in the nonimplanted eye (column 2). IR stimulation of the nonimplanted eye did not result in cortical activity any greater than baseline cortical activity (column 3).

Noninvasive Device Performance Monitoring

The HK Loop ERG electrode placed on the cornea was used to record the voltage change as the device was activated with varying light intensities. These measurements were recorded in three rabbits before euthanasia and three rabbits immediately after euthanasia; no systematic difference was observed between before and after euthanasia experiments. A typical device activation signal is shown in the top graph of Figure 7 as IR light was pulsed for 10 ms while varying the IR power from 0 to 3.4 mW/mm^2. The trough-to-peak corneal potential amplitudes resulting from device activation increases logarithmically with increased IR laser power, as shown in the bottom six graphs of Figure 7. Although the corneal potential amplitude varied greatly between recordings, the shape of the relationship between corneal potential and irradiance remained consistent.

DISCUSSION

The purpose of this study was to determine the feasibility of a photovoltaic nanowire–based subretinal prosthesis to drive visual responses in a rabbit model. We demonstrate that the subretinal nanowire prosthesis can generate visual cortical

FIGURE 6. The average focal VEP amplitude (94.88 ± 43.3 µV) was significantly higher than EEP (54.17 ± 33.4 µV), IR only (24.07 ± 22.1 µV), and baseline cortical activity (23.22 ± 17.2 µV) amplitudes. Average EEP amplitude differed significantly from IR stimulation of the nonimplanted eye and baseline. Cortical potentials measured when stimulating the nonimplanted eye with IR light did not generated amplitudes significantly different from baseline cortical activity. *Boxes* indicate 25th/75th percentiles, and *dotted lines* are the ranges of amplitude values.

signals powered only with infrared light by recording EEPs in anesthetized rabbit visual cortex. Furthermore, as a negative control, we showed that IR light of the same intensity does not cause any stimulation of photoreceptors in intact retina of the nonimplanted eye, indicating that visual cortical signals are the result of electrical stimulation of the retina by the prosthetic. Initially the negative control recordings were taken by focusing the IR laser on retina further away from the device in the implanted eye; however, we detected some device activation from the corneal electrode recording, likely due to scattering light from the high intensity laser. Therefore, the nonimplanted eye was used to prevent scattered light from confounding the experiment. In addition, we demonstrate that subretinal implantation of the prosthetic device can be successfully performed while preserving the function of the overlying retina by recording focal VEPs in response to visible light, and we show how corneal potential recordings can be used to validate device activation. Together these results provide evidence for the viability of a subretinal nanowire prosthetic approach to vision restoration.

Measuring VEPs and EEPs in an in vivo animal model is a standard preclinical practice for most retinal prosthesis research groups; however, there is considerable variability in how results are presented due to a lack of standardized methods. Even so, there are still specific response hallmarks that are common between groups. For example, although some groups present a fast positive peak followed by a long negative trough,[26,27,30] whereas other groups present a fast negative trough followed by a long positive peak,[20–22,24,25,28,31] there is still a typical waveform pattern of a short latency voltage deflection (either negative or positive) followed by a rapid reversal in voltage that slowly decays back to baseline. This typical waveform pattern is qualitatively similar to a classical VEP waveform, with one major difference being that EEP latencies are generally shorter than VEP latencies.[24,27] It is theorized that the shorter latencies of electrical retinal stimulation are a result of bypassing the relatively slow phototransduction cascade of the photoreceptors by directly stimulating inner retinal neurons. Our results are consistent with other groups, showing a shorter N1 EEP latency than VEP N1 and a characteristic waveform that fits the overall interpretation of EEPs.

Vertical silicon nanowires are highly efficient at using the photovoltaic effect to convert light into electrical stimulation. The p-n junction within the silicon photodiode is responsible for the photovoltaic conversion of light to current; no other material used in the fabrication of the device can contribute to the photocurrent given the band gap energies of each material.[32–35] In this study, we used 3.4-mW/mm^2 IR light to activate the silicon nanowires operating in photovoltaic mode. This level of irradiance is 20 times lower than thermal safety limits for 10-ms pulses of 852-nm light.[38] Past work from our group has shown that applying bias to the nanowire devices
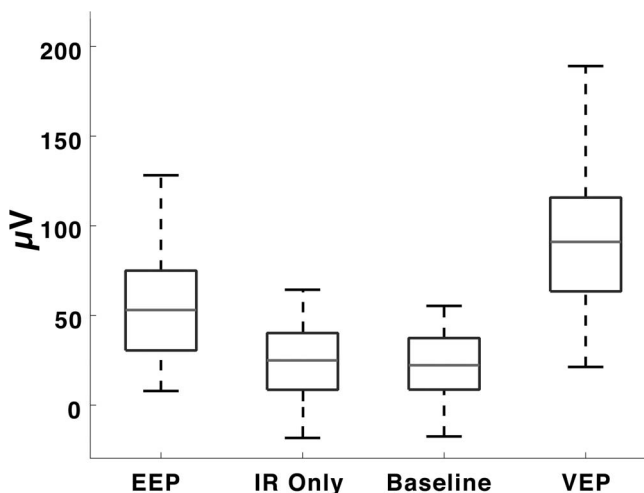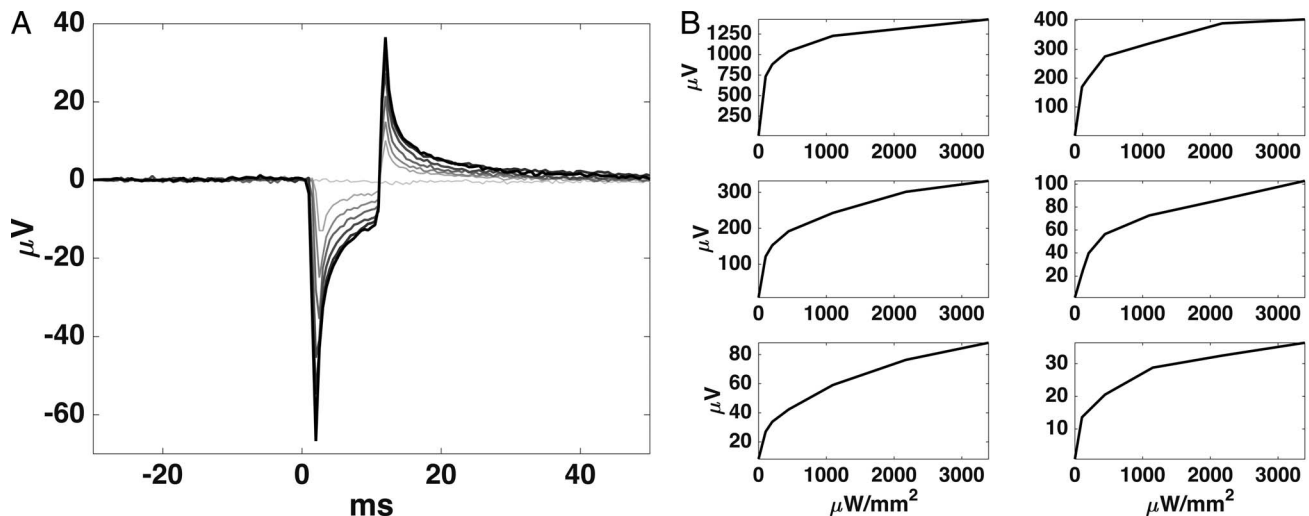
FIGURE 7. The device activation signal recorded from an electrode on the cornea increased in amplitude as the IR light power activating the device was increased. (A) The larger graph shows a typical device activation signal waveform. (B) The smaller six graphs show the relationship between device activation corneal potentials and IR power in three live (*left*) and three euthanized (*right*) rabbits. Note that the absolute voltage amplitude varied due to variations in electrode placement and tissue impedances.

greatly increases the gain, which can be exploited to further decrease the irradiance required to reach stimulation threshold.[17] Regardless, these experiments serve as an important proof of principle in the design of subretinal nanowire prosthetics. Future experiments will explore the relationship between light intensity, charge injection, stimulation frequency, and the stimulation threshold to elicit EEPs.

The corneal potential recorded from the ERG electrode served as a control to confirm device activation. Corneal potential increased logarithmically as the IR laser power was increased, consistent with a logarithmic increase in charge output. This is congruent with similar work from Lorach et al., which reported increased corneal potential amplitude with increased illumination area.[20] As expected, the absolute amplitudes of corneal potentials are not directly comparable between subjects due to variations in electrode placement, tissue impedances, or anatomical differences, but relative potential over a range of irradiance provides a qualitative measure of device performance.[39] The corneal waveform could also be modulated by decreasing or increasing the laser pulse duration (data not shown), which can be used as another measure of validating device performance. Corneal monitoring of device activation is an important control measure in clinical testing because it can be noninvasively used as a method to verify device function over the lifetime of the implant.

The optically activated nanowire-based prosthesis offers several significant advantages to other retinal prosthetic strategies currently being pursued. The nanowire design allows the integration of photodetection and neural stimulation into each pixel. This allows for individual pixels to be optically addressed, which greatly simplifies the form factor and packaging requirements for a retinal prosthesis and obviates the need for hard wired connections to the pixels of an external camera,[40] which is a daunting engineering challenge. It also eliminates the need for a complicated integrated circuit for each pixel as in the case for prosthetics making use of an intraocular CMOS sensor.[41] With the nanowire-based prosthesis, a large number of high density electrodes can be placed in a small surgically tractable package. The device tested here covered approximately a 3- × 4-mm area of retina providing more than 17° of visual field while containing 1512 electrodes at 50-µm spacing. This design

may offer advantages versus the individually wired 60 electrodes in the Argus II or the 378 optically addressed electrodes in the Pixium PRIMA in terms of electrode density and visual field and with a simpler electrical component packaging strategy compared with the Alpha AMS. Although estimation of visual acuity from retinal spacing alone is challenging, it is widely assumed that increasing pixel density will lead to an increase in visual acuity. From sampling theory, a 50-µm pixel pitch roughly corresponds to a best theoretical acuity of approximately 20/400.[42–44] This compares favorably with other devices on the market or in clinical testing in terms of array spacing.[41,45–47] Taken together the photovoltaic nanowire device described here represents a novel advance in the field of retinal prosthetics.

CONCLUSIONS

In this paper, we demonstrated how a passive, unpowered nanowire photodiode array can transduce light into an electrical stimulation that evokes a physiologic response in the rabbit visual cortex. We previously showed ex vivo that we can further boost the sensitivity of the system by providing bias power.[17] In future experiments, we will harness this effect to enable phototransduction under dimmer light conditions by applying external power to the nanowires to increase the dynamic range of electrical stimulation and reduce the light intensity required to elicit a response.

Inc. (F, C, R); **G. Cauwenberghs**, Nanovision Biosciences, Inc. (S); **W.R. Freeman**, Nanovision Biosciences, Inc. (C) P

References

1. Hartong DT, Berson EL, Dryja TP. Retinitis pigmentosa. *Lancet*. 2006;368:1795–1809.

2. Wong WL, Su X, Li X, et al. Global prevalence of age-related macular degeneration and disease burden projection for 2020 and 2040: a systematic review and meta-analysis. *Lancet Global Health*. 2014;2:e106–e116.

3. Stone JL, Barlow WE, Humayun MS, de Juan E Jr, Milam AH. Morphometric analysis of macular photoreceptors and ganglion cells in retinas with retinitis pigmentosa. *Arch Ophthalmol*. 1992;110:1634–1639.

4. Jones BW, Kondo M, Terasaki H, Lin Y, McCall M, Marc RE. Retinal remodeling. *Jpn J Ophthalmol*. 2012;56:289.

5. Edwards TL, Cottriall CL, Xue K, et al. Assessment of the electronic retinal implant alpha AMS in restoring vision to blind patients with end-stage retinitis pigmentosa. *Ophthalmology*. 2018;125:432–443.

6. Gekeler K, Bartz-Schmidt KU, Sachs H, et al. Implantation, removal and replacement of subretinal electronic implants for restoration of vision in patients with retinitis pigmentosa. *Curr Opin Ophthalmol*. 2018;29:239–247.

7. Pixium Vision Press Release. Pixium Vision announces CE market approval of IRIS® II, its first bionic vision system. Available at: http://www.pixium-vision.com/en/media/press-releases. Accessed June 1, 2018.

8. da Cruz L, Dorn JD, Humayun MS, et al. Five-year safety and performance results from the Argus II Retinal Prosthesis System clinical trial. *Ophthalmology*. 2016;123:2248–2254.

9. ClinicalTrials.gov. Identifier NCT03629899, retina implant alpha AMS in blind patients with retinitis pigmentosa. Available at: https://clinicaltrials.gov/ct2/show/NCT03629899. Accessed August 14, 2018.

10. ClinicalTrials.gov. Identifier NCT03333954: feasibility study of compensation for blindness with the PRIMA system in patients with dry age related macular degeneration (PRIMA FS). Available at: https://www.clinicaltrials.gov/ct2/show/NCT03333954. Accessed November 6, 2017.

11. Boinagrov D, Lei X, Goetz G, et al. Photovoltaic pixels for neural stimulation: circuit models and performance. *IEEE Trans Biomed Circuits Syst*. 2016;10:85–97.

12. Goetz GA, Palanker DV. Electronic approaches to restoration of sight. *Rep Prog Phys*. 2016;79:096701.

13. Lorach H, Goetz G, Smith R, et al. Photovoltaic restoration of sight with high visual acuity. *Nat Med*. 2015;21:476–482.

14. Mathieson K, Loudin J, Goetz G, et al. Photovoltaic retinal prosthesis with high pixel density. *Nature Photonics*. 2012;6:391–397.

15. Loudin JD, Simanovskii DM, Vijayraghavan K, et al. Optoelectronic retinal prosthesis: system design and performance. *J Neural Eng*. 2007;4:S72–S84.

16. Palanker D, Vankov A, Huie P, Baccus S. Design of a high-resolution optoelectronic retinal prosthesis. *J Neural Eng*. 2005;2:S105–S120.

17. Ha S, Khraiche M, Akinin A, et al. Towards high-resolution retinal prostheses with direct optical addressing and inductive telemetry. *J Neural Eng*. 2016;13:056008.

18. Grosberg LE, Ganesan K, Goetz GA, et al. Activation of ganglion cells and axon bundles using epiretinal electrical stimulation. *J Neurophysiol*. 2017;118:1457.

19. Norcia AM, Appelbaum LG, Ales JM, Cottereau BR, Rossion B. The steady-state visual evoked potential in vision research: a review. *J Vis*. 2015;15(6):4.

20. Lorach H, Goetz G, Mandel Y, et al. Performance of photovoltaic arrays in-vivo and characteristics of prosthetic vision in animals with retinal degeneration. *Vis Res*. 2015;111:142–148.

21. Lorach H, Lei X, Galambos L, et al. Interactions of prosthetic and natural vision in animals with local retinal degeneration. *Vis Neurosci*. 2015;56:7444–7450.

22. Yan Y, Sui X, Liu W, et al. Spatial characteristics of evoked potentials elicited by a MEMS microelectrode array for suprachoroidal-transretinal stimulation in a rabbit. *Graefe's Arch Clin Exp Ophthalmol*. 2015;253:1515–1528.

23. Nayagam DAX, Williams RA, Allen PJ, et al. Chronic electrical stimulation with a suprachoroidal retinal prosthesis: a preclinical safety and efficacy study. *PLoS One*. 2014;9:e97182.

24. Mandel Y, Goetz G, Lavinsky D, et al. Cortical responses elicited by photovoltaic subretinal prostheses exhibit similarities to visually evoked potentials. *Nature Commun*. 2013;4:1980.

25. Shah HA, Montezuma SR, Rizzo JF III. In vivo electrical stimulation of rabbit retina: effect of stimulus duration and electrical field orientation. *Exp Eye Res*. 2006;83:247–254.

26. Nakauchi K, Fujikado T, Kanda H, et al. Transretinal electrical stimulation by an intrascleral multichannel electrode array in rabbit eyes. *Graefe's Arch Clin Exp Ophthalmol*. 2005;243:169–174.

27. Rizzo JF, Goldbaum S, Shahin M, Denison TJ, Wyatt J. In vivo electrical stimulation of rabbit retina with a microfabricated array: strategies to maximize responses for prospective assessment of stimulus efficacy and biocompatibility. *Restorat Neurol Neurosci*. 2004;22:429–443.

28. Yamauchi Y, Franco LM, Jackson DJ, et al. Comparison of electrically evoked cortical potential thresholds generated with subretinal or suprachoroidal placement of a microelectrode array in the rabbit. *J Neural Eng*. 2005;2:S48–S56.

29. Walter P, Heimann K. Evoked cortical potentials after electrical stimulation of the inner retina in rabbits. *Graefe's Arch Clin Exp Ophthalmol*. 2000;238:315–318.

30. Nadig MN. Development of a silicon retinal implant: cortical evoked potentials following focal stimulation of the rabbit retina with light and electricity. *Clin Neurophysiol*. 1999;110:1545–1553.

31. Chow AY, Chow VY. Subretinal electrical stimulation of the rabbit retina. *Neurosci Lett*. 1997;225:13–16.

32. Sun K, Kargar A, Park N, et al. Compound semiconductor nanowire solar cells. *IEEE J Sel Topics Quantum Electron*. 2011;17:1033–1049.

33. Soci C, Zhang A, Bao XY, Kim H, Lo Y, Wang D. Nanowire photodetectors. *J Nanosci Nanotechnol*. 2010;10:1430–1449.

34. Cui Y, Lieber CM. Functional nanoscale electronic devices assembled using silicon nanowire building blocks. *Science*. 2001;291:851–853.

35. Brewer SH, Wicaksana D, Maria JP, Kingon AI, Franzen S. Investigation of the electrical and optical properties of iridium oxide by reflectance FTIR spectroscopy and density functional theory calculations. *Chem Physics*. 2005;313:25–31.

36. Khraiche ML, Emam SE, Akinin A, Cauwenberghs G, Freeman W, Silva GA. *Visual Evoked Potential Characterization of Rabbit Animal Model for Retinal Prosthesis Research*. Osaka, Japan, July 3-7, 2013. 35th Annual International Conference of the IEEE Engineering in Medicine and Biology Society (EMBC), 2013.

37. Nuboer JFW, Moed PJ. Increment-threshold spectral sensitivity in the rabbit. *J Comparat Physiol*. 1983;151:353–358.

38. Lorach H, Wang JD, Lee Y, Dalal R, Huie P, Palanker D. Retinal safety of near infrared radiation in photovoltaic restoration of sight. *Biomed Opt Express*. 2016;7:13–21.

39. Bosse B, Zrenner E, Wilke R. Standard ERG equipment can be used to monitor functionality of retinal implants. *Conf Proc IEEE Eng Med Biol Soc*. 2011;1089–1092.

40. Weiland JD, Humayun MS. Retinal prosthesis. *IEEE Trans Biomed Eng*. 2014;61:1412–1424.

41. Stingl K, Schippert R, Bartz-Schmidt KU, et al. Interim results of a multicenter trial with the new electronic subretinal implant alpha AMS in 15 patients blind from inherited retinal degenerations. *Front Neurosci*. 2017;11:445.

42. Damle S, Lo YH, Freeman WR. High visual acuity retinal prosthesis: understanding limitations and advancements toward functional prosthetic vision. *Retina*. 2017;37:1423–1427.

43. Stronks HC, Dagnelie G. The functional performance of the Argus II retinal prosthesis. *Exp Rev Med Devices*. 2014;11:23–30.

44. Moghadam GK, Wilke R, Suaning GJ, Lovell NH, Dokos S. Quasi-monopolar stimulation: a novel electrode design configuration for performance optimization of a retinal neuroprosthesis. *PLoS One*. 2013;8:e73130.

45. Humayun MS, Dorn JD, Cruz LD, et al. Interim results from the International Trial of Second Sight's Visual Prosthesis. *Ophthalmology*. 2012;119:779–788.

46. Dagnelie G, Christopher P, Arditi A, et al. Performance of real-world functional vision tasks by blind subjects improves after implantation with the Argus® II retinal prosthesis system. *Clin Exp Ophthalmol*. 2017;45:152–159.

47. Ayton LN, Blamey PJ, Guymer RH, et al. First-in-human trial of a novel suprachoroidal retinal prosthesis. *PLoS One*. 2014;9:e115239.